iScience

Article

Dioxygen reductase heterogeneity is crucial for robust aerobic growth physiology of *Escherichia coli*

Graphical abstract

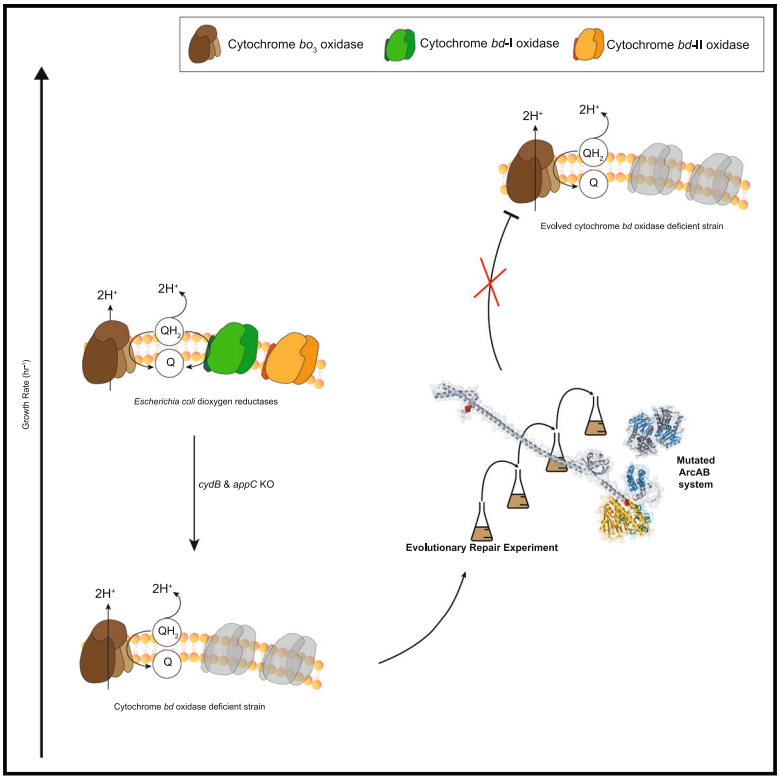

Highlights

- Deficiency of cytochrome *bd* oxidases impairs the aerobic growth of *E. coli*
- Loss of ArcAB function alleviates growth defect in cytochrome *bd* oxidase-deficient *E. coli*
- Adaptive rewiring results in collateral compromise in the bacterial stress response pathway

Authors

Anjali V. Patil, Akshay M. Shirsath, Amitesh Anand

Correspondence

amitesh.anand@tifr.res.in

In brief

Biological sciences; Biochemistry; Microbiology

Patil et al., 2024, iScience *27*, 111498
December 20, 2024
https://doi.org/10.1016/j.isci.2024.111498

CellPress

iScience

CellPress
OPEN ACCESS

Article

Dioxygen reductase heterogeneity is crucial for robust aerobic growth physiology of *Escherichia coli*

Anjali V. Patil,[1] Akshay M. Shirsath,[1] and Amitesh Anand[1,2,*]
[1]Department of Biological Sciences, Tata Institute of Fundamental Research, Mumbai, Maharashtra 400005, India
[2]Lead contact
*Correspondence: amitesh.anand@tifr.res.in
https://doi.org/10.1016/j.isci.2024.111498

SUMMARY

The development of a system to leverage molecular oxygen for energy-efficient pathways required several molecular adaptations. The enzymatic reduction of dioxygen to water is one such prominent evolutionary molecular trait. Microbes evolved several enzymes capable of reducing dioxygen and, interestingly, retained multiples of them in their genomes. While their structure and biochemical functions are well-studied, understanding their degeneracy and co-operativity in the system remains elusive.

We used genetic engineering and evolutionary repair approaches to examine the impact of the high oxygen affinity cytochrome bd oxidase deficiency in Escherichia coli aerobic growth. We found a crucial role of cytochrome bd oxidases in the robustness of aerobic physiology. Evolutionary repair experiments alleviated growth defects in bd oxidase-deficient strains by ArcAB system dysregulation at the cost of impaired stress response pathways. Energy generation pathways are potential antimicrobial targets, and understanding collateral phenotypes is crucial in designing therapeutic approaches that reduce antimicrobial resistance development.

INTRODUCTION

Oxygen, which colloquially synonymizes life, was a nonexistent molecule in primitive Earth's environment. The rise of oxygen in the environment necessitated several molecular changes in microbial physiology to withstand oxygen toxicity and exploit this high reduction potential molecule for evolving a superior energetics system.[1] The evolution of dioxygen reductases (O_2REDs) is suggested to be an adaptive mechanism to reduce oxygen to water, which later became a hallmark of aerobic respiration.[2]

There are several types of O_2REDs that differ in the redox centers and, consequently, in their reduction potentials.[3] The primary role of the O_2REDs is to facilitate the aerobic flow of electrons in the electron transport system (ETS), and the range of reduction potential enables their functioning in a wide range of oxygen partial pressures. Two major classes of O_2REDs are heme center-based and heme-copper hybrid center-based oxidoreductases.[4] Heme-center-based oxidoreductases are more widely distributed than heme-copper center-based oxidoreductases; often, both O_2REDs are present within the same bacterium.[5,6] Dioxygen reductases appear to be functionally substitutable for bacteria in an aerobic environment.[7–10] The significance of accumulating multiple O_2REDs in an otherwise conservative bacterial genome is incomprehensible.[11]

Escherichia coli, a facultative anaerobe, has both the O_2REDs: (i) cytochrome bo_3 oxidase consisting of heme *b*, heme o_3, and copper redox centers and (ii) two types of cytochrome *bd* oxidases (*bd*-I and *bd*-II) consisting of heme *b* and heme *d* redox centers (Figure 1A).[12] The two O_2REDs differ in their oxygen affinities. Cytochrome bo_3 oxidase has lower oxygen affinity and is reported to be the primary O_2RED in aerobic environments.[13] Cytochrome *bd* oxidases have higher oxygen affinity and are observed to be majorly expressed in microaerobic environments.[14] These O_2REDs have different abilities to support proton motive force (PMF) generation. Cytochrome bo_3 oxidase yields a PMF of $2H^+/e^-$ by pumping a proton and translocating another vectorially. In contrast, cytochrome *bd* oxidases do not actively pump protons but still contribute to a PMF of $1H^+/e^-$ through the vectorial translocation of protons.[15,16] The deficiency of neither cytochrome bo_3 oxidase nor cytochrome *bd* oxidase is reported to impact the aerobic growth of *E. coli*.[7,17,18]

Interestingly, cytochrome *bd* oxidases are also implicated in redox homeostasis, pathogenesis, and antimicrobial tolerance, suggesting a broader role of these oxidases in bacterial pathophysiology.[20–24] Therefore, cytochrome *bd* oxidases are being explored as potential antimicrobial targets. To understand cytochrome *bd* oxidases' contributions to aerobic growth physiology and bacterial adaptive response to their loss, we genetically engineered an *E. coli* strain lacking both cytochrome *bd* oxidases. We performed an evolutionary repair experiment to resolve the proximal and distal response to the loss of high oxygen affinity oxidases in an aerobic environment.[25] We found[1]: while there is a minor growth defect for the loss of individual O_2REDs, the deficiency of both cytochrome *bd* oxidases decreases the aerobic growth significantly,[2] evolutionary repair experiments could restore the growth of the strain,[3] the evolved strains alleviate

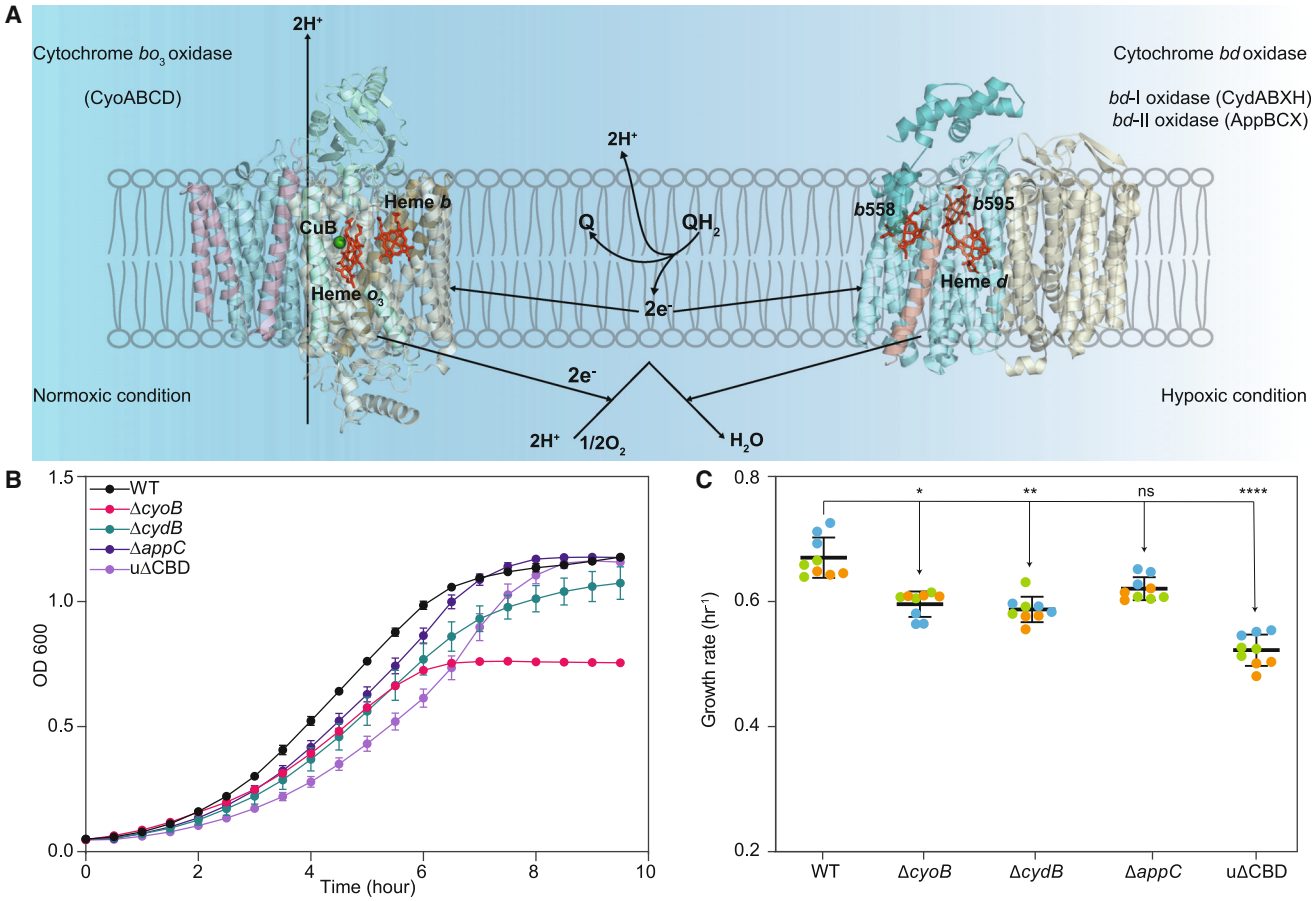

Figure 1. Contribution of dioxygen reductases in aerobic growth of *E. coli*

(A) Schematic representation of dioxygen reductase diversity in *E. coli*. *E. coli* has a low oxygen affinity cytochrome bo_3 oxidase and two high oxygen affinity *bd* oxidases: *bd*-I and *bd*-II (only *bd*-II shown above for representation purposes). Cytochrome bo_3 oxidase pumps one proton and translocates another vectorially to create a proton motive force of $2H^+/e^-$ effectively. Cytochrome *bd* oxidases contribute to a proton motive force of $1H^+/e^-$ by vectorial translocation. (Color scheme - cytochrome bo_3 oxidase: CyoB-Peach, CyoA-Green, CyoC-Blue, CyoD-Pink; cytochrome *bd*-II oxidase: AppB-Green, AppC-Peach, AppX-Orange).

(B) Influence of dioxygen reductase deficiency on the aerobic growth of *E. coli*. The growth curve shows a mean of three biological replicates (with three technical replicates each), and the error bars show the standard error of the mean.

(C) Growth rates of dioxygen reductase deficient *E. coli* strains grown in aerobic conditions. The plot shows the mean of three biological replicates (each with three technical replicates (in the same color)), and the error bars show the standard deviation. The Kruskal-Wallis test was performed to determine the significance of growth rate differences compared to wild-type (WT).[19] Cytochrome bo_3 oxidase deficient (Δ*cyoB*), cytochrome *bd*-I oxidase deficient (Δ*cydB*), cytochrome *bd*-II oxidase deficient (Δ*appC*), unevolved cytochrome *bd* oxidase deficient (uΔCBD). See also Figures S1 and S2.

ArcAB repression for aerobic growth optimization,[4] the evolved strains have better carbon utilization efficiency and oxidative phosphorylation dependency, and[5] the evolutionary growth optimization sensitizes the strain to agents generating reactive oxygen species. We report the bioenergetic superiority and associated tradeoffs of cytochrome *bd* oxidase-deficient strain. We demonstrate the criticality of O_2RED degeneracy in robust aerobic physiology.

RESULTS AND DISCUSSION

Influence of dioxygen reductase deficiencies on aerobic growth and evolutionary repair

O_2REDs complete the aerobic flow of electrons through ETS by transferring them to oxygen. While cytochrome bo_3 oxidase is reported to be the preferred O_2RED,[26] we examined the influence of all three O_2REDs of *E. coli* on aerobic growth. We engineered four strains differing in their O_2RED compositions: (a) cytochrome bo_3 oxidase deficient (Δ*cyoB*), (b) cytochrome *bd*-I oxidase deficient (Δ*cydB*), (c) cytochrome *bd*-II oxidase deficient (Δ*appC*), and (d) cytochrome *bd* oxidase deficient (Δ*cydB*Δ*appC*, hereafter labeled as ΔCBD; we will be using uΔCBD specifically for unevolved/starting strain) (Figure S1). The deficiency of any individual O_2RED resulted in a similar drop in exponential growth compared to the wild-type (WT) (Figures 1B and 1C). Notably, consistent with the report of reduced biomass, Δ*cyoB* enters the stationary phase earlier than other strains.[27] Δ*cydB* and Δ*appC* showed similar growth profiles, although *bd*-I oxidase seems more critical than *bd*-II oxidase. However, it is the deletion of both cytochrome *bd* oxidases that caused the most significant

A

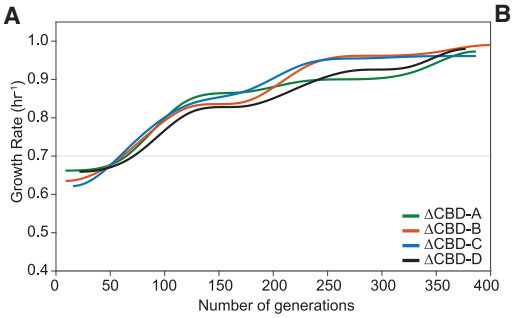

B

Strain	Mutations		
eΔCBD-A	Δ82 bp *pyrE-rph*	Deletion: *mtgA*, *elbB*, *arcZ*, ***arcB***, *yhcC*, *gltB*, *gltD*, *gltF*, *yhcA*, *yhcD*, *yhcE*	
eΔCBD-B		*rpoB* H526Y	*arcA* R67C
eΔCBD-C	Δ1 bp *pyrE-rph*	*rpoC* H419P	*arcB* A8V
eΔCBD-D		*rpoC* D622G	*arcB* I290S

Figure 2. Genetic basis for the growth optimization of cytochrome *bd* oxidase-deficient *E. coli*

(A) Aerobic growth optimization of cytochrome *bd* oxidase-deficient strain by evolutionary repair experiment.

(B) List of genes mutated in the evolved ΔCBD strains compared to the unevolved ΔCBD strain. See also Table S1 and Figure S3.

growth retardation (Figures 1B and 1C). Thus, while *bd*-I and *bd*-II oxidases are substitutable, at least one of the cytochrome *bd* oxidases is required in an aerobic environment. As expected, complementing the *appC* gene in ΔCBD improves its aerobic growth (Figure S2).

Since uΔCBD has functional cytochrome bo_3 oxidase, which is reported to be the primary aerobic oxidase, we wanted to examine whether the strain can recover its full growth potential.[26] Therefore, we performed an evolutionary repair experiment by continuously passaging ΔCBD in an aerobic growth condition until the increase in growth rate plateaued. We observed similar evolution trajectories for this strain's four independently evolved lineages (eΔCBD-A-D) (Figure 2A; Table S1). In about 350 generations, all four lineages achieved growth rates ($\sim$0.9 h^{-1}) similar to a wild-type strain that evolved under the same conditions.[28,29] This growth rate improvement indicated the existence of compensatory mechanisms in cytochrome *bd* oxidase-deficient strain.

Genetic basis for evolutionary repair of cytochrome *bd* oxidase deficiency in *E. coli*

The restoration of stress-induced growth defects in bacteria is frequently attributable to some adaptive genetic changes. We performed the genome sequencing of the ΔCBD strains to determine the genetic basis of their growth improvement. Each evolved lineage acquired mutations that have been characterized to improve the growth of *E. coli* on the M9 minimal medium (Figure 2B). Three of the eΔCBD strains mutated RNA polymerase subunits. These mutations enhance the transcriptional rate and, in turn, improve growth.[28,30] Intergenic mutations of *pyrE-rph* are also associated with enhancing growth by alleviating orotate phosphoribosyltransferase deficiency and restoring pyrimidine biosynthesis.[28] These mutations are acquired by a glucose minimal media-optimized strain (GMOS), a WT strain evolved under a similar condition.[28]

Along with these well-characterized growth-promoting mutations, all evolved lineages acquired mutations in the ArcAB two-component system (Figure 2B). This anoxic redox control (Arc) system consists of a sensor kinase (ArcB) and a response regulator (ArcA).[31] The ArcAB system regulates respiro-fermentative metabolism.[32] Among several genes repressed by this system, the genes coding for cytochrome bo_3 oxidase are notable in the context of this study. The functioning of this oxidase should be relevant in the absence of cytochrome *bd* oxidases. We, therefore, explored the nature of the observed mutations. ArcAB is reported to be constitutively expressed, and we also observed no significant difference in the expression level of these genes[33] (Figure S3). In eΔCBD-A, an approximately 16 kb part of the genome was deleted, encompassing the *arcB* gene; therefore, we do not observe the expression of this gene (Figures 2B and S3).

The complete deletion of the *arcB* gene in the eΔCBD-A strain indicated that the mutations observed in the evolved strains potentially result in a loss of function of the ArcAB system. The evolved lineages C and D had point mutations in the *arcB* gene, while lineage B had a point mutation in the *arcA* gene. We investigated the effect of these mutations on the ArcA and ArcB proteins by analyzing amino acid properties, sequence homology, and overall structural stability.[34–37] In the eΔCBD-B strain, we identified the ArcA-R67C mutation in the N-terminal response regulator domain (Figure 3A). This mutation replaces a charged, hydrophilic residue with a neutral, hydrophobic residue, potentially destabilizing the protein and impairing its function. The mutations in eΔCBD-C and eΔCBD-D strains led to the formation of two ArcB protein variants: A8V-ArcB and I290S-ArcB (Figure 3B). The A8V mutation, located in the transmembrane domain, introduces a valine residue. Valine has a lower propensity to contribute to a helical structure and can disrupt protein folding.[38,39] The I290S variant introduces a serine residue, which is less hydrophobic than the wild-type residue, potentially affecting the protein's intrinsic interactions. Notably, the I290S mutation is near a key residue involved in the ArcB phosphorelay mechanism (H292),[33] likely impacting the protein's functionality. To experimentally support the interpretation from protein structure simulation, we introduced the WT copy of the *arcB* gene in evolved lineage D harboring a point mutation in this gene. We observed a growth defect upon the restoration of *arcB* (Figure S4).

To strengthen the causality of the *arcB* mutations in improving the growth of uΔCBD, we engineered ArcB deficiency in uΔCBD by knocking out the *arcB* gene. The uΔCBDΔ*arcB* strain showed growth improvement compared to the uΔCBD strain (Figure 3C),

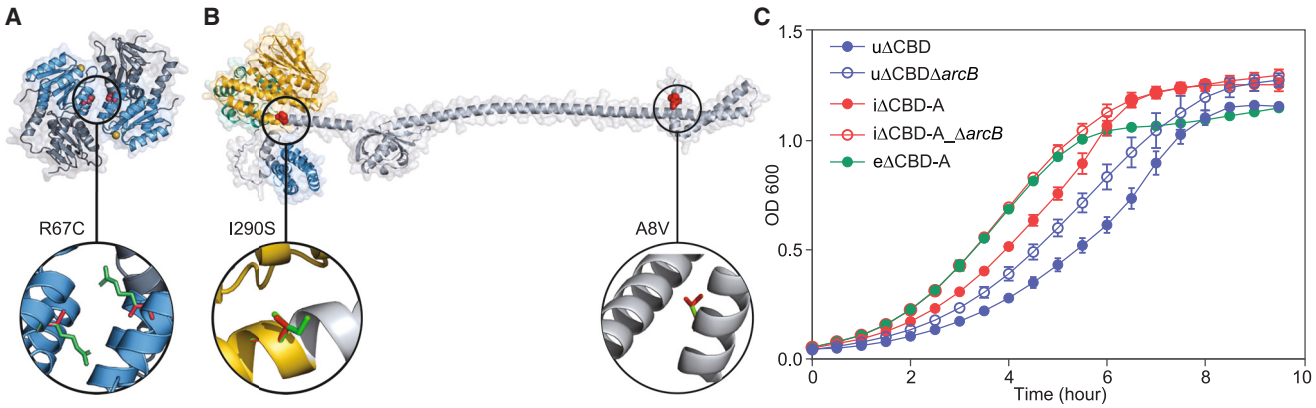

Figure 3. Validation of causality and nature of mutation in evolved cytochrome *bd* oxidase-deficient *E. coli*

(A) The point mutation observed in the eΔCBD-B strain mapped on the ArcA protein from *E. coli* (AlphaFold3 structure rendered using sequence from Uniprot ID P0AEC3) (Color scheme: Response regulatory domain-Blue, Magnesium ions-Orange).

(B) The point mutations observed in the eΔCBD-C and eΔCBD-D strains mapped on the ArcB protein from *E. coli* (AlphaFold3 structure rendered using sequence from Uniprot ID P0A9Q1) (Color scheme: Histidine kinase domain-Yellow, Response regulatory domain-Green, Hpt domain-Blue). In the zoomed-in inset of Figures 3A and 3B, green represents wild-type amino acid residue, while red represents mutant amino acid residue.

(C) Effect of *arcB* gene deletion on the growth profile of ΔCBD strains. The growth curve shows a mean of three biological replicates (with three technical replicates each), and the error bars show the standard error of the mean. See also Table S2 and Figures S4 and S5.

suggesting that *arcB* loss of function is responsible for improving the growth. Interestingly, the deletion of the *arcB* gene in the WT strain showed growth retardation, reestablishing the benefit of *arcB* loss of function being specific to the ΔCBD strain (Figure S5). However, the eΔCBD-A strain showed better growth than uΔCBDΔ*arcB*, potentially due to additional contributions from mutations responsible for facilitating faster growth on the M9 minimal medium. We probed the additive interactions between these two classes of mutations by picking an intermediate strain (iΔCBD) from the evolutionary lineage that had media-responsive mutations only (Table S2). We then knocked out *arcB* in iΔCBD-A to create iΔCBD-A_Δ*arcB.* The iΔCBD-A_Δ*arcB* strain grew similarly to eΔCBD-A (Figure 3C). The growth rate trend of uΔCBD < uΔCBDΔ*arcB* < iΔCBD-A < eΔCBD-A ∼ iΔCBD-A_Δ*arcB* established the additive effect of ArcAB and media-responsive mutations in improving the growth of uΔCBD.

Metabolic adjustments underlying the growth optimization of cytochrome *bd* oxidase-deficient strain

Genetic adaptation acts through metabolic rewiring to improve phenotypes. The ArcAB system influences a wide range of bacterial physiology, with respiration being a primary target. ArcAB inhibits the expression of cytochrome bo_3 oxidase and promotes the expression of cytochrome *bd* oxidases.[40] We examined the expression levels of genes of subunit I (*cyoB*) and II (*cyoA*) of cytochrome bo_3 oxidase in the ΔCBD strains (Figure 4A). uΔCBD strain showed a significant increase in the expression as compared to WT. We used an evolved strain of WT as a reference to examine expression response to an increase in growth rate. GMOS decreased the expression of *cyoAB*.[29] Interestingly, in the eΔCBD strain, the expression of bo_3 oxidase was maintained to a level similar to uΔCBD, suggesting that the loss of function of ArcAB might alleviate repression on the expression of cytochrome bo_3 oxidase. While we observed a trend toward higher expression of *cyoAB* in eΔCBD, the difference was not statistically significant.

We estimated a panel of respiratory exometabolites (glucose, acetate, lactate, succinate, and formate) in the growth medium to probe the metabolic rewiring in the evolved strains. We observed an increased glucose uptake rate in strains with higher growth rates (GMOS and eΔCBD-A) (Table S3). However, unlike GMOS, the eΔCBD strain did not show a proportional increase in acetate secretion rate. The eΔCBD strain showed a lower carbon loss in the form of acetate with no detectable rise in other fermentation metabolites (Figure 4B; Table S3). The most efficient carbon utilization route is to flux the acetate to the TCA cycle, which feeds into the ETS. We compared the oxygen consumption profile of the evolved and unevolved ΔCBD strains to assess if the rise in ETS operation is responsible for efficient carbon utilization. The eΔCBD strain showed a higher oxygen consumption per biomass than uΔCBD (Figure 4C). These results indicate that the growth improvement of the uΔCBD strain is driven by efficient oxidative phosphorylation and not due to reliance on acetate overflow.

Collateral phenotypes of cytochrome *bd* oxidase-deficiency

Glucose is a respiro-fermentative metabolite; therefore, glucose-based energetics can have contributions from both respiratory and fermentative metabolism. We then used succinate as the carbon source to compare the contributions of respiratory energetics toward the growth of ΔCBD strains. We observed the retention of growth superiority of eΔCBD compared to uΔCBD when fermentative energetics are restricted (Figures 4D and S6A).

Beyond regulating respiration, the ArcAB system contributes to redox homeostasis, and its dysregulation can affect

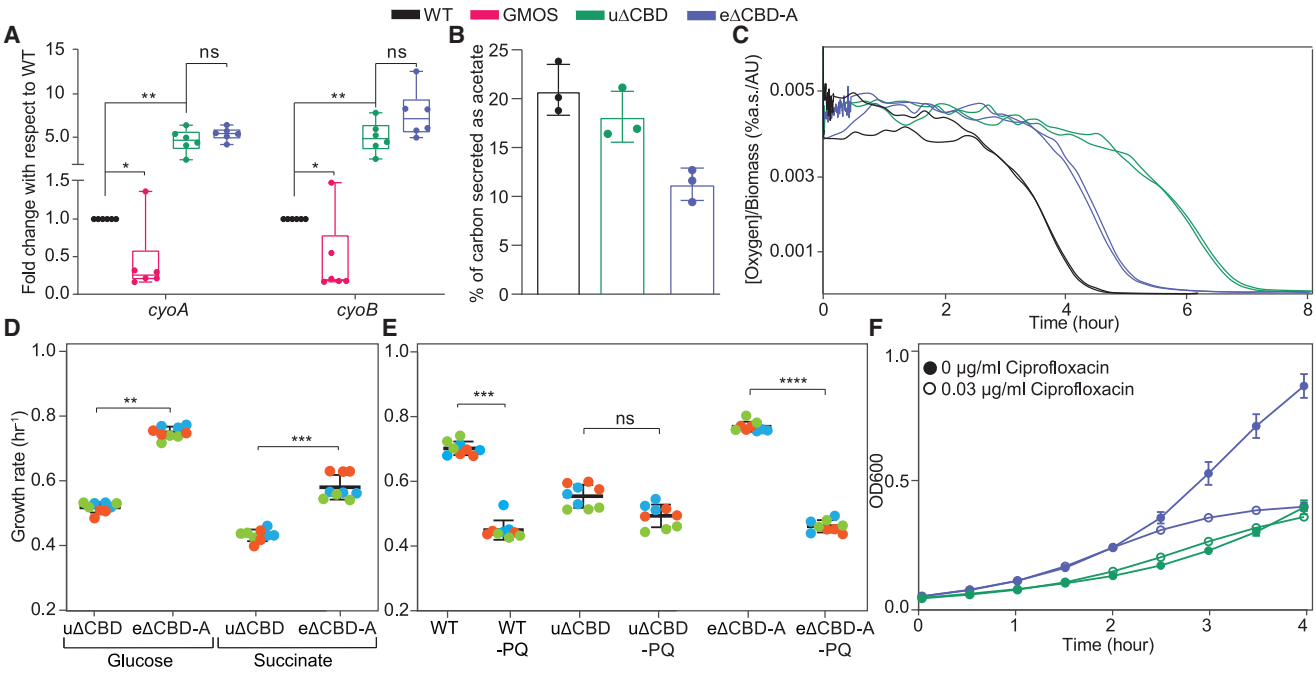

Figure 4. Metabolic basis for the growth optimization of cytochrome *bd* oxidase-deficient *E. coli*

(A) Relative expression of the cytochrome bo_3 oxidase genes (*cyoA* and *cyoB*) in GMOS and ΔCBD strains with respect to WT. All six replicate values are displayed. Whiskers represent the maximum and minimum data points, while the solid line inside the boxplots represents the median. Significance was determined using the Mann-Whitney test.[41]

(B) The percentage of carbon secreted as acetate is determined using the strains' corresponding glucose uptake rate and acetate secretion rate.

(C) Estimation of oxygen uptake normalized to biomass in the strains determined using fluorescence sensor-based oxygen measurements. Two independent replicates are displayed independently. Growth rates of cytochrome *bd* oxidase-deficient *E. coli* in the following media conditions: (D) M9 minimal medium supplemented with succinate as sole carbon source and (E) M9 minimal medium supplemented with 4 g/L glucose and 5μM Paraquat (PQ). The plot shows the mean of three biological replicates (each with three technical replicates (in the same color)), and the error bars show the standard deviation. The Kruskal-Wallis test was performed to determine the significance of growth rate differences.[19] Panel (D) and (E) share the y axis description.

(F) Growth profiles of cytochrome *bd* oxidase-deficient *E. coli* in M9 minimal medium supplemented with 4 g/L glucose and ciprofloxacin. The growth curve shows a mean of three biological replicates (with three technical replicates each), and the error bars show the standard error of the mean. See also Table S3 and Figure S6.

stress response capacities.[31] We examined the sensitivity of ΔCBD strains to superoxide by treating them with paraquat. uΔCBD showed a lower reactive oxygen species (ROS) sensitivity compared to the WT strain. The evolved strain showed the most significant drop in growth rate on paraquat exposure among these strains, suggesting eΔCBD to be more sensitive to superoxide (Figures 4E and S6B). Notably, such differences in ROS sensitivity could also arise due to the differences in their growth rates. Such fitness tradeoffs can further compromise tolerance to antibiotics working by generating ROS. We probed this hypothesis by challenging the strains with ciprofloxacin, a fluoroquinolone antibiotic known to elevate cellular ROS in eliciting its bactericidal activity.[42] We observed a relatively higher sensitivity to ciprofloxacin in the evolved ΔCBD strain (Figures 4F and S6C). Interestingly, the SOS response induced by ciprofloxacin may cause some mutagenic changes, which might have a confounding impact on the data interpretation.[43]

Our observations suggest a critical role of cytochrome *bd* oxidase even in aerobic physiology and strengthen its candidacy as an antibiotic development target. However, the underlying adaptive rewiring is crucial in designing therapeutic approaches. We are restricting this study to the proposition that antibiotics targeting cytochrome *bd* oxidase in combination with ROS-generating antibiotics may limit resistant strain development. Parallely, the carbon-efficient nature of the evolved strains encourages the proposal of the strains' bioproduction applications since the reduction in carbon loss as acetate has been reported to improve recombinant protein production.[44–46]

Limitations of the study

The study aimed to investigate the importance of cytochrome *bd* oxidase deficiency on the aerobic growth of *E. coli* and the compensatory response to the deficiency of these oxidases. Following up on the relative contributions and cooperation between various dioxygen reductases in aerobic conditions can provide crucial insights into bioenergetics. Also, the upregulation of cytochrome bo_3 oxidase expression in the unevolved strain presents an intriguing avenue for future research, especially to uncover the molecular mechanisms behind this adaptive response. Further, the bioproduction and biotherapeutic claims of the study remain to be validated.

RESOURCE AVAILABILITY

Lead contact

Further information and requests for reagents may be directed to, and will be fulfilled by, the corresponding author, Dr. Amitesh Anand (amitesh.anand@tifr.res.in).

Material availability

All bacterial strains generated in this study are available from the lead contact with a completed Materials Transfer Agreement.

Data and code availability

- DNAseq data supporting this study are deposited in the NCBI Sequence Read Archive (PRJNA1127851).
- This article does not report any original code.
- Any additional information required to reanalyze the data reported in this article is available from the lead contact upon request.

ACKNOWLEDGMENTS

This work was supported by the DAE-Tata Institute of Fundamental Research Grant (19P0120) and DBT-Ramalingaswami Fellowship (21X432) to Amitesh Anand. We thank Prof. Bernhard Palsson (Systems Biology Research Group, University of California, San Diego) for sharing the evolutionary repair experiment resources. We would like to express our heartfelt gratitude to Mr. Sebastian S. Cocioba (Binomica Labs, New York) for providing the pECXA-FuGFP+KanR plasmid used in this study.

AUTHOR CONTRIBUTIONS

A.A. designed the study. A.A. and A.P. performed the experiments. A.A., A.P., and A.S. analyzed the data and wrote the article.

DECLARATION OF INTERESTS

The authors declare no competing interests.

STAR★METHODS

Detailed methods are provided in the online version of this paper and include the following:

- KEY RESOURCES TABLE
- EXPERIMENTAL MODEL AND SUBJECT DETAILS
  - Bacterial strains and growth conditions
- METHOD DETAILS
  - Genetic complementation of mutants
  - Evolutionary repair experiment
  - DNA resequencing
  - Structure preparation and visualization in PyMol
  - Protein structure simulation to perform mutation analysis
  - RNA isolation and qPCR
  - Phenotype characterization
- QUANTIFICATION AND STATISTICAL ANALYSIS

SUPPLEMENTAL INFORMATION

Supplemental information can be found online at https://doi.org/10.1016/j.isci.2024.111498.

Received: June 17, 2024
Revised: July 28, 2024
Accepted: November 26, 2024
Published: November 28, 2024

REFERENCES

1. Sessions, A.L., Doughty, D.M., Welander, P.V., Summons, R.E., and Newman, D.K. (2009). The continuing puzzle of the great oxidation event. Curr. Biol. *19*, R567–R574.
2. Falkowski, P.G. (2006). Evolution. Tracing oxygen's imprint on earth's metabolic evolution. Science *311*, 1724–1725.
3. Poole, R.K. (1983). Bacterial cytochrome oxidases. A structurally and functionally diverse group of electron-transfer proteins. Biochim. Biophys. Acta *726*, 205–243.
4. Thöny-Meyer, L. (1997). Biogenesis of respiratory cytochromes in bacteria. Microbiol. Mol. Biol. Rev *61*, 337–376. https://doi.org/10.1128/mmbr.61.3.337-376.1997.
5. Borisov, V.B., Siletsky, S.A., Paiardini, A., Hoogewijs, D., Forte, E., Giuffrè, A., and Poole, R.K. (2021). Bacterial Oxidases of the Cytochrome Family: Redox Enzymes of Unique Structure, Function, and Utility As Drug Targets. Antioxidants Redox Signal. *34*, 1280–1318.
6. Borisov, V.B., Gennis, R.B., Hemp, J., and Verkhovsky, M.I. (2011). The cytochrome bd respiratory oxygen reductases. Biochim. Biophys. Acta *1807*, 1398–1413.
7. Au, D.C., Lorence, R.M., and Gennis, R.B. (1985). Isolation and characterization of an Escherichia coli mutant lacking the cytochrome o terminal oxidase. J. Bacteriol. *161*, 123–127.
8. Kana, B.D., Weinstein, E.A., Avarbock, D., Dawes, S.S., Rubin, H., and Mizrahi, V. (2001). Characterization of the cydAB-encoded cytochrome bd oxidase from Mycobacterium smegmatis. J. Bacteriol. *183*, 7076–7086.
9. Fischer, M., Falke, D., Naujoks, C., and Sawers, R.G. (2018). Cytochrome Oxidase Has an Important Role in Sustaining Growth and Development of Streptomyces coelicolor A3(2) under Oxygen-Limiting Conditions. J. Bacteriol. *200*, e00239-18. https://doi.org/10.1128/JB.00239-18.
10. Winstedt, L., Yoshida, K., Fujita, Y., and von Wachenfeldt, C. (1998). Cytochrome bd biosynthesis in Bacillus subtilis: characterization of the cydABCD operon. J. Bacteriol. *180*, 6571–6580.
11. McKay, L.S., Spandrio, A.R., Johnson, R.M., Sobran, M.A., Marlatt, S.A., Mote, K.B., Dedloff, M.R., Nash, Z.M., Julio, S.M., and Cotter, P.A. (2024). Cytochrome Oxidase Requirements in Bordetellareveal Insights into Evolution towards Life in the Mammalian Respiratory Tract. PLoS Pathog *20*, e1012084. https://doi.org/10.1101/2024.02.29.582880.
12. Unden, G., and Bongaerts, J. (1997). Alternative respiratory pathways of Escherichia coli: energetics and transcriptional regulation in response to electron acceptors. Biochim. Biophys. Acta Bioenerg. *1320*, 217–234.
13. Kita, K., Konishi, K., and Anraku, Y. (1984). Terminal oxidases of Escherichia coli aerobic respiratory chain. I. Purification and properties of cytochrome b562-o complex from cells in the early exponential phase of aerobic growth. J. Biol. Chem. *259*, 3368–3374.
14. Kita, K., Konishi, K., and Anraku, Y. (1984). Terminal oxidases of Escherichia coli aerobic respiratory chain. II. Purification and properties of cytochrome b558-d complex from cells grown with limited oxygen and evidence of branched electron-carrying systems. J. Biol. Chem. *259*, 3375–3381.
15. Anand, A., Patel, A., Chen, K., Olson, C.A., Phaneuf, P.V., Lamoureux, C., Hefner, Y., Szubin, R., Feist, A.M., and Palsson, B.O. (2022). Laboratory evolution of synthetic electron transport system variants reveals a larger metabolic respiratory system and its plasticity. Nat. Commun. *13*, 3682.
16. Borisov, V.B., Murali, R., Verkhovskaya, M.L., Bloch, D.A., Han, H., Gennis, R.B., and Verkhovsky, M.I. (2011). Aerobic respiratory chain of Escherichia coli is not allowed to work in fully uncoupled mode. Proc. Natl. Acad. Sci. USA *108*, 17320–17324.
17. Green, G.N., and Gennis, R.B. (1983). Isolation and characterization of an Escherichia coli mutant lacking cytochrome d terminal oxidase. J. Bacteriol. *154*, 1269–1275.

18. Website https://www.microbiology.ubc.ca/sites/default/files/roles/drupal_ungrad/JEMI/17/13.3G.pdf.
19. McKight, P.E., and Najab, J. (2010). Kruskal-Wallis Test. In The Corsini Encyclopedia of Psychology (John Wiley & Sons, Ltd), p. 1.
20. Al-Attar, S., Yu, Y., Pinkse, M., Hoeser, J., Friedrich, T., Bald, D., and de Vries, S. (2016). Cytochrome bd Displays Significant Quinol Peroxidase Activity. Sci. Rep. *6*, 27631.
21. Forte, E., Nastasi, M.R., and Borisov, V.B. (2022). Preparations of Terminal Oxidase Cytochrome bd-II Isolated from Escherichia coli Reveal Significant Hydrogen Peroxide Scavenging Activity. Biochemistry *87*, 720–730.
22. Hammer, N.D., Reniere, M.L., Cassat, J.E., Zhang, Y., Hirsch, A.O., Indriati Hood, M., and Skaar, E.P. (2013). Two heme-dependent terminal oxidases power Staphylococcus aureus organ-specific colonization of the vertebrate host. mBio *4*, e00241-13. https://doi.org/10.1128/mBio.00241-13.
23. Endley, S., McMurray, D., and Ficht, T.A. (2001). Interruption of the cydB Locus inBrucella abortus Attenuates Intracellular Survival and Virulence in the Mouse Model of Infection. J. Bacteriol. *183*, 2454–2462. https://doi.org/10.1128/jb.183.8.2454-2462.2001.
24. Mascolo, L., and Bald, D. (2020). Cytochrome bd in Mycobacterium tuberculosis: A respiratory chain protein involved in the defense against antibacterials. Prog. Biophys. Mol. Biol. *152*, 55–63.
25. LaBar, T., Phoebe Hsieh, Y.-Y., Fumasoni, M., and Murray, A.W. (2020). Evolutionary Repair Experiments as a Window to the Molecular Diversity of Life. Curr. Biol. *30*, R565–R574.
26. Cotter, P.A., Chepuri, V., Gennis, R.B., and Gunsalus, R.P. (1990). Cytochrome o (cyoABCDE) and d (cydAB) oxidase gene expression in Escherichia coli is regulated by oxygen, pH, and the fnr gene product. J. Bacteriol. *172*, 6333–6338.
27. Richhardt, J., Luchterhand, B., Bringer, S., Büchs, J., and Bott, M. (2013). Evidence for a key role of cytochrome bo3 oxidase in respiratory energy metabolism of Gluconobacter oxydans. J. Bacteriol. *195*, 4210–4220.
28. LaCroix, R.A., Sandberg, T.E., O'Brien, E.J., Utrilla, J., Ebrahim, A., Guzman, G.I., Szubin, R., Palsson, B.O., and Feist, A.M. (2015). Use of adaptive laboratory evolution to discover key mutations enabling rapid growth of Escherichia coli K-12 MG1655 on glucose minimal medium. Appl. Environ. Microbiol. *81*, 17–30.
29. Anand, A., Chen, K., Catoiu, E., Sastry, A.V., Olson, C.A., Sandberg, T.E., Seif, Y., Xu, S., Szubin, R., Yang, L., et al. (2020). OxyR Is a Convergent Target for Mutations Acquired during Adaptation to Oxidative Stress-Prone Metabolic States. Mol. Biol. Evol. *37*, 660–667.
30. Conrad, T.M., Frazier, M., Joyce, A.R., Cho, B.-K., Knight, E.M., Lewis, N.E., Landick, R., and Palsson, B.Ø. (2010). RNA polymerase mutants found through adaptive evolution reprogram Escherichia coli for optimal growth in minimal media. Proc. Natl. Acad. Sci. USA *107*, 20500–20505.
31. Brown, A.N., Anderson, M.T., Bachman, M.A., and Mobley, H.L.T. (2022). The ArcAB Two-Component System: Function in Metabolism, Redox Control, and Infection. Microbiol. Mol. Biol. Rev. *86*, e0011021.
32. Alexeeva, S., de Kort, B., Sawers, G., Hellingwerf, K.J., and de Mattos, M.J. (2000). Effects of limited aeration and of the ArcAB system on intermediary pyruvate catabolism in Escherichia coli. J. Bacteriol. *182*, 4934–4940.
33. Malpica, R., Sandoval, G.R.P., Rodríguez, C., Franco, B., and Georgellis, D. (2006). Signaling by the arc two-component system provides a link between the redox state of the quinone pool and gene expression. Antioxidants Redox Signal. *8*, 781–795.
34. Venselaar, H., Te Beek, T.A.H., Kuipers, R.K.P., Hekkelman, M.L., and Vriend, G. (2010). Protein structure analysis of mutations causing inheritable diseases. An e-Science approach with life scientist friendly interfaces. BMC Bioinf. *11*, 548.
35. Abramson, J., Adler, J., Dunger, J., Evans, R., Green, T., Pritzel, A., Ronneberger, O., Willmore, L., Ballard, A.J., Bambrick, J., et al. (2024). Accurate structure prediction of biomolecular interactions with AlphaFold 3. Nature *630*, 493–500.
36. Dehouck, Y., Grosfils, A., Folch, B., Gilis, D., Bogaerts, P., and Rooman, M. (2009). Fast and accurate predictions of protein stability changes upon mutations using statistical potentials and neural networks: PoPMuSiC-2.0. Bioinformatics *25*, 2537–2543.
37. Landau, M., Mayrose, I., Rosenberg, Y., Glaser, F., Martz, E., Pupko, T., and Ben-Tal, N. (2005). ConSurf 2005: the projection of evolutionary conservation scores of residues on protein structures. Nucleic Acids Res. *33*, W299–W302.
38. Lyu, P.C., Liff, M.I., Marky, L.A., and Kallenbach, N.R. (1990). Side chain contributions to the stability of alpha-helical structure in peptides. Science *250*, 669–673.
39. O'Neil, K.T., and DeGrado, W.F. (1990). A thermodynamic scale for the helix-forming tendencies of the commonly occurring amino acids. Science *250*, 646–651.
40. Rolfe, M.D., Ter Beek, A., Graham, A.I., Trotter, E.W., Asif, H.M.S., Sanguinetti, G., de Mattos, J.T., Poole, R.K., and Green, J. (2011). Transcript profiling and inference of Escherichia coli K-12 ArcA activity across the range of physiologically relevant oxygen concentrations. J. Biol. Chem. *286*, 10147–10154.
41. McKnight, P.E., and Najab, J. (2010). Mann-Whitney U Test. In The Corsini Encyclopedia of Psychology (John Wiley & Sons, Ltd), p. 1.
42. Goswami, M., Mangoli, S.H., and Jawali, N. (2006). Involvement of reactive oxygen species in the action of ciprofloxacin against Escherichia coli. Antimicrob. Agents Chemother. *50*, 949–954.
43. Pourahmad Jaktaji, R., and Pasand, S. (2016). Overexpression of SOS genes in ciprofloxacin resistant Escherichia coli mutants. Gene *576*, 115–118.
44. Gecse, G., Labunskaite, R., Pedersen, M., Kilstrup, M., and Johanson, T. (2024). Minimizing acetate formation from overflow metabolism in : comparison of genetic engineering strategies to improve robustness toward sugar gradients in large-scale fermentation processes. Front. Bioeng. Biotechnol. *12*, 1339054.
45. Vemuri, G.N., Eiteman, M.A., and Altman, E. (2006). Increased recombinant protein production in Escherichia coli strains with overexpressed water-forming NADH oxidase and a deleted ArcA regulatory protein. Biotechnol. Bioeng. *94*, 538–542.
46. Nizam, S.A., Zhu, J., Ho, P.Y., and Shimizu, K. (2009). Effects of arcA and arcB genes knockout on the metabolism in Escherichia coli under aerobic condition. Biochem. Eng. J. *44*, 240–250.
47. Thomason, L.C., Costantino, N., and Court, D.L. (2007). E. coli genome manipulation by P1 transduction. Curr. Protoc. Mol. Biol. Chapter *1*, 1–7.
48. Baba, T., Ara, T., Hasegawa, M., Takai, Y., Okumura, Y., Baba, M., Datsenko, K.A., Tomita, M., Wanner, B.L., and Mori, H. (2006). Construction of Escherichia coli K-12 in-frame, single-gene knockout mutants: the Keio collection. Mol. Syst. Biol. *2*, 2006.0008.
49. Blazanin, M. (2024). gcplyr: an R package for microbial growth curve data analysis. BMC Bioinf. *25*, 232.
50. Engler, C., Kandzia, R., and Marillonnet, S. (2008). A one pot, one step, precision cloning method with high throughput capability. PLoS One *3*, e3647.

STAR★METHODS

KEY RESOURCES TABLE

REAGENT or RESOURCE	SOURCE	IDENTIFIER
Bacterial and virus strains		
Escherichia coli K12 MG1655	ATCC	700926
Escherichia coli K12 MG1655_Δ*cyoB*	This study	N/A
Escherichia coli K12 MG1655_Δ*cydB*	This study	N/A
Escherichia coli K12 MG1655_Δ*appC*	This study	N/A
Escherichia coli K12 MG1655_Δ*cydB*Δ*appC*	This study	N/A
Escherichia coli K12 MG1655_Δ*cydB*Δ*appC*_A13F16I1R1	This study	A13F16I1R1
Escherichia coli K12 MG1655_Δ*cydB*Δ*appC*_A14F16I1R1	This study	A14F16I1R1
Escherichia coli K12 MG1655_Δ*cydB*Δ*appC*_A15F16I1R1	This study	A15F16I1R1
Escherichia coli K12 MG1655_Δ*cydB*Δ*appC*_A16F16I1R1	This study	A16F16I1R1
Escherichia coli K12 MG1655_Δ*cydB*Δ*appC*_A13F58I1R1	This study	A13F58I1R1
Escherichia coli K12 MG1655_Δ*cydB*Δ*appC*_A14F60I1R1	This study	A14F60I1R1
Escherichia coli K12 MG1655_Δ*cydB*Δ*appC*_A15F57I1R1	This study	A15F57I1R1
Escherichia coli K12 MG1655_Δ*cydB*Δ*appC*_A16F56I1R1	This study	A16F56I1R1
Escherichia coli K12 MG1655_Δ*cydB*Δ*appC*Δ*arcB*	This study	N/A
Escherichia coli K12 MG1655_Δ*arcB*	This study	N/A
Escherichia coli K12 MG1655_Δ*cydB*Δ*appC*_A13F16I1R1_Δ*arcB*	This study	N/A
Chemicals, peptides, and recombinant proteins		
$CaCl_2.2H_2O$	Sigma Aldrich	C3306
$MgSO_4.7H_2O$	SRL	1344116
Na_2HPO_4	Sigma Aldrich	S9763
KH_2PO_4	Sigma Aldrich	P5655
NaCl	MP Bio	194848
NH_4Cl	Sigma Aldrich	A4515
$FeCl_3.6H_2O$	Sigma Aldrich	F2877
$ZnCl_2$ anhydrous	Sigma Aldrich	Z1052
$CoCl_2.6H_2O$	Sigma Aldrich	C8661
$Na_2MoO_4.2H_2O$	Sigma Aldrich	M1651
$CuCl_2.2H_2O$	Sigma Aldrich	C3279
H_3BO_3	USB	76324
Concentrated HCl	Sigma Aldrich	H1758
Glucose	Sigma Aldrich	49139
Sodium succinate dibasic	Sigma Aldrich	14160
Luria-Bertani broth	Himedia	M575
Luria-Bertani agar	Himedia	M1151
Kanamycin	Sigma Aldrich	K1377
Ampicillin	Sigma Aldrich	A9518
Ciprofloxacin	Sigma Aldrich	17850
Paraquat	Sigma Aldrich	36541
BsaI-HFv2	NEB	R3733S
rCutsmart 10X	NEB	B6004S
TRIzol reagent	Thermo Fisher Scientific	15596018
Chloroform	SDFCL	3771OUR
Absolute ethanol	Honeywell	32221

(*Continued on next page*)

Continued

REAGENT or RESOURCE	SOURCE	IDENTIFIER
H_2SO_4	Sigma Aldrich	40325
Sodium acetate	Sigma Aldrich	791741
Sodium lactate	Sigma Aldrich	71718
Sodium formate	Sigma Aldrich	798630
Critical commercial assays		
Nucleospin Tissue kit	Macherey Nagel	740952.50
Nextera XT kit	Illumina	FC-131–1024
First Strand cDNA synthesis kit	Thermo Scientific	18091050
SsoAdvanced Universal SYBR Green Supermix	BioRad	1725270
Deposited data		
DNAseq data	NCBI Sequence Read Archive	PRJNA1127851
Oligonucleotides		
k1: CAGTCATAGCCGAATAGCCT	Sigma Aldrich	Customised
cyoB FP: CTAGCGAATACAACCAGGTG	Sigma Aldrich	Customised
cydB FP: CGAACTCGTCACTGACCGCA	Sigma Aldrich	Customised
appC FP: TTTGGTCGACTCTGCGCAGC	Sigma Aldrich	Customised
appC RP: CCAGACCTGGTTGCCTTCCC	Sigma Aldrich	Customised
appC FP with BsaI extension: TATAGGTCTCGAA TGTGGGATGTCATTGATTT	Sigma Aldrich	Customised
appC RP with BsaI extension: TATAGGTCTCAAA GCTTACCCCTGTTGCTGCGTCG	Sigma Aldrich	Customised
arcB FP with BsaI extension: TATAGGTCTCGAAT GAAGCAAATTCGTCTGC	Sigma Aldrich	Customised
arcB RP with BsaI extension: TATAGGTCTCAAAG CTCATTTTTTAGTGGCTTTTG	Sigma Aldrich	Customised
Software and algorithms		
Graph Pad Prism	Version 10.0.2	Graph pad.com
gcplyr	https://github.com/mikeblazanin/gcplyr	N/A
PyMol	Version 3.0	N/A
AlphaFold3	https://doi.org/10.1038/s41586-024-07487-w	N/A

EXPERIMENTAL MODEL AND SUBJECT DETAILS

Bacterial strains and growth conditions

Bacterial strains and primers used in this study are listed in the key resources table. *Escherichia coli* K12 MG1655 (ATCC 700926) was used as the wild-type strain. Knockout strains were generated using the P1 phage transduction method, with Keio collection strains as donors for gene knockout cassettes.[47,48] All the growth assays were performed using the Tecan Spark multimode microplate reader at 37°C and atmospheric oxygen partial pressure using 96 well plate with 200μL culture per well. Three biological replicates (each with three technical replicates) were performed for each experiment. Unless stated otherwise, M9 minimal medium supplemented with 4 g/L glucose was used for bacterial growth. For the growth profiling with media variation, the concentration of succinate used is calculated according to the carbon equivalence of 4 g/L glucose while paraquat and ciprofloxacin were added to M9 minimal medium supplemented with 4 g/L glucose at a final concentration of 5 μM and 0.03 μg/mL, respectively. Growth rate calculations are done using gcplyr: an R package for microbial growth curve data analysis.[49]

METHOD DETAILS

Genetic complementation of mutants

The plasmids, pECXA-*appC* and pECXA-*arcB*, were constructed using golden gate assembly.[50] The plasmids were made using pECXA-FuGFP+KanR, kindly shared by Sebastian S. Cocioba (Binomica Labs, New York), containing minimal constitutive promoter J23100. FuGFP+KanR was replaced with the gene of interest (oligonucleotides are listed in the key resources table). Growth

characterization of the transformed strains was performed as mentioned in the preceding section, with ampicillin in the medium as a selection marker for the plasmid.

Evolutionary repair experiment

The evolutionary repair experiment was performed using four independent replicates of the Δ*cydB*Δ*appC* strain. Cultures were serially propagated in M9 minimal medium supplemented with 4 g/L glucose at 37°C and atmospheric oxygen partial pressure, using an automated system that passed the cultures to fresh tubes once they had reached an OD_{600} of 0.3 (Tecan 26 Sunrise plate reader, equivalent to an OD_{600} of ~1 on a traditional spectrophotometer with a 1 cm path length). The cultures were well-mixed for proper aeration. Cultures were always maintained in excess nutrient conditions assessed by non-tapering exponential growth. The laboratory evolution was performed for a sufficient interval to allow the cells to reach their growth rate plateau.

DNA resequencing

DNA resequencing was performed on a clone from the endpoints of evolved strains. Total DNA was sampled from an overnight culture and immediately centrifuged for 5 min at 8,000 r.p.m. The supernatant was decanted, and the cell pellet was frozen at −80°C. Genomic DNA was isolated using a Nucleospin Tissue kit (Macherey Nagel 740952.50) following the manufacturer's protocol, including treatment with RNase A. Resequencing libraries were prepared using a Nextera XT kit (Illumina FC-131–1024) following the manufacturer's protocol. Libraries were run on a HiSeq and/or NextSeq (Illumina).

Sequencing reads were filtered and trimmed using the software AfterQC version 0.9.623. The breseq bioinformatics pipeline version 0.31.1 was used to map sequencing reads and identify mutations relative to an *E. coli* K-12 MG1655 reference genome (NC_000913.3) amended to reflect the starting strain best.

Structure preparation and visualization in PyMol

Protein structures of cytochrome bo_3 oxidase (PDB ID: 8F68) and cytochrome *bd*-II oxidase (PDB ID: 7OY2) of *E. coli* K-12 were acquired from the Protein DataBank (PDB). These structures were rendered using PyMol to facilitate detailed visualization.

Protein structure simulation to perform mutation analysis

The sequence for wild-type ArcA and ArcB proteins of *E. coli* K-12 was retrieved from the UniProt database under the identifier numbers P0A9Q1 and P0AEC3, respectively. The protein structure for ArcA and ArcB was created using AlphaFold3[35] and used to analyze the impact of mutations. PyMol was used to introduce mutated residues and create the mutant protein structures.

RNA isolation and qPCR

Bacteria were grown in an M9 minimal medium supplemented with 4 g/L glucose till their mid-exponential phase. The culture was harvested and immediately processed for RNA isolation. The cells were dissolved in a TRIzol and incubated at 65°C for 15 min. RNA was obtained in an aqueous layer upon the addition of chloroform, which was then precipitated using chilled isopropanol. This RNA pellet was washed with alcohol and finally resuspended in DEPC-treated water. RNA was quantified using a nano spectrophotometer before being frozen at −80°C for later use. cDNA synthesis was performed using Thermo Scientific RevertAid First Strand cDNA synthesis kit using random hexamer primer, according to the manufacturer's protocol. Quantitative real-time PCR was carried out with BioRad SsoAdvanced Universal SYBR Green Supermix in CFX Opus 96 real-time PCR system (BioRad).

Phenotype characterization

Culture density was measured at 600 nm absorbance with a spectrophotometer and correlated to cell biomass. Samples for exometabolite estimation were filtered through a 0.22 μm filter (PVDF, Millipore) and measured using refractive index detection by HPLC (Agilent 12600 Infinity) with a Bio-Rad Aminex HPX87-H ion exclusion column. The HPLC method was the following: injection volume of 10 μL and 5 mM H_2SO_4 mobile phase set to a flow rate and temperature of 0.5 mL/min and 45°C, respectively, for a run time of 20 min per sample.

The oxygen uptake of each culture was determined by measuring the depletion of dissolved oxygen using the Presens oxygen sensor system (SFR vario). The cultures grown in M9 minimal medium supplemented with 4 g/L glucose at 37°C/300 r.p.m in the SFR vario sensor shake flasks were used to measure oxygen and biomass changes.

QUANTIFICATION AND STATISTICAL ANALYSIS

Prism (GraphPad) version 10 was used for quantification and generation of plots. All experiments in this study were performed at least in triplicate. The growth curves show a mean of three biological replicates (with three technical replicates each), and the error bars show the standard error of the mean. The growth rate plots show the mean of three biological replicates (each with three technical replicates), and the error bars show the standard deviation. The Kruskal-Wallis test was performed to determine the significance of growth rate differences. The significance for the relative expression of the cytochrome bo_3 oxidase genes was determined using the Mann-Whitney test. The figure legends of each plot mention the statistical details and tests used.